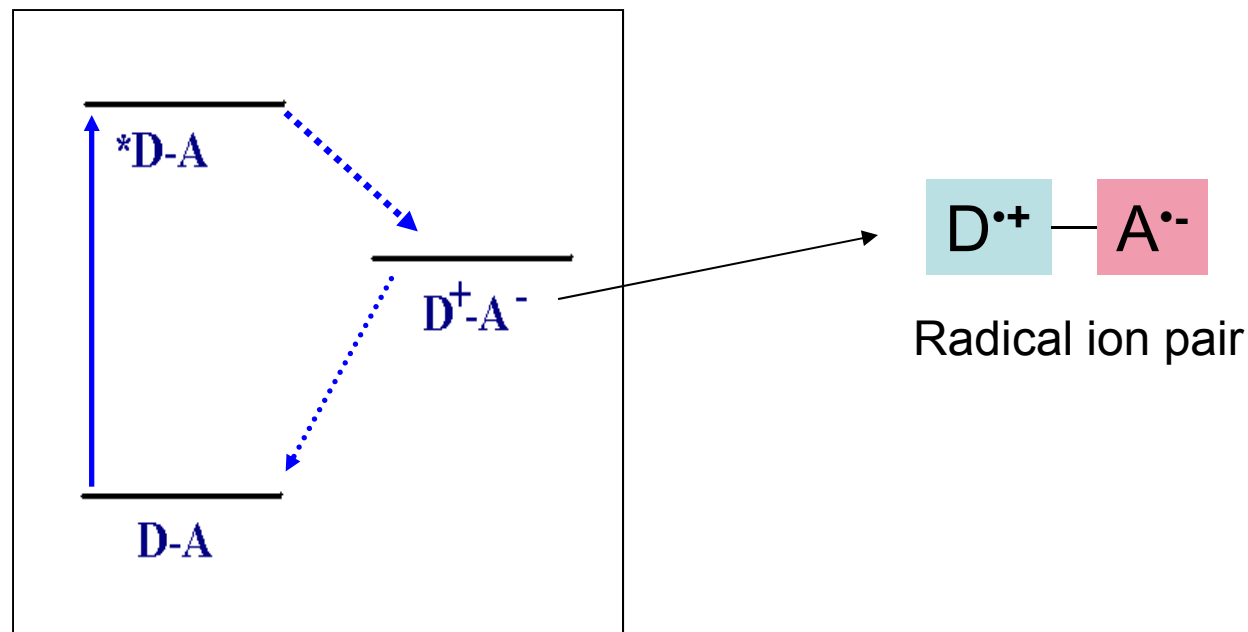


Molecular Photonics

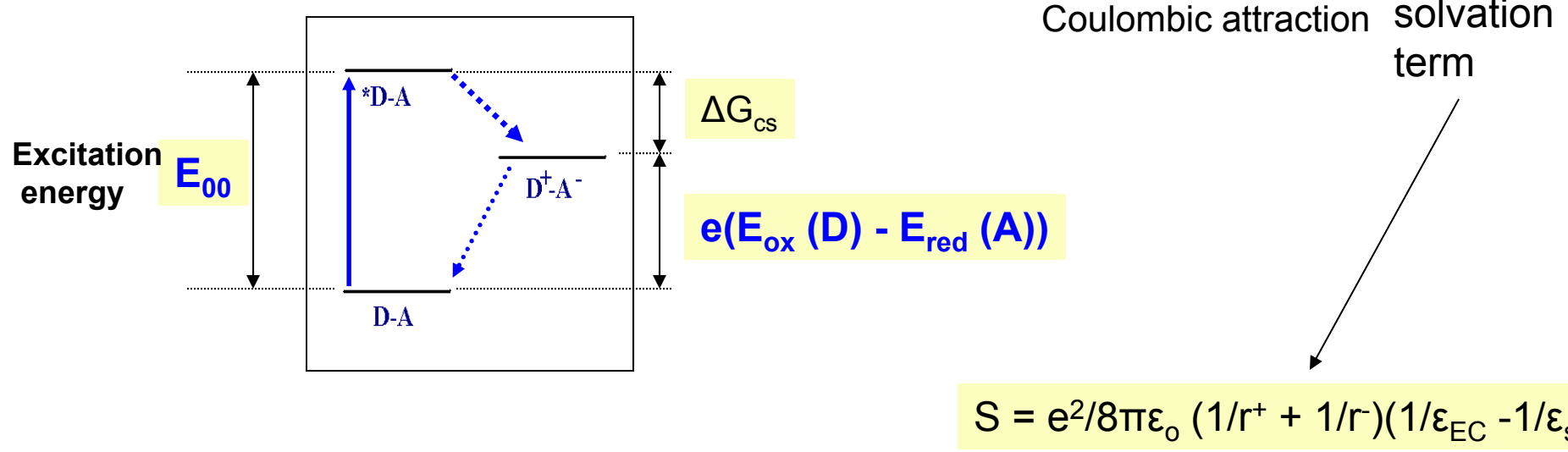
Lecture 6.

Photoinduced Electron Transfer



Driving force for photoinduced electron transfer: Rehm-Weller equation for Thermodynamic analysis

$$\Delta G_{cs} = \frac{e(E_{ox}(D) - E_{red}(A))}{\text{Coulombic attraction}} - \frac{e^2/4\pi\epsilon_0\epsilon_s R_c}{\text{solvation term}} - S$$



$E_{ox}(D)$ and $E_{red}(A)$ - Redox potentials (obtained electrochemically)

e = elementary charge, $e=1$ if units are eV

R_c = distance between D and A

ϵ_{EC} - Dielectric constant of a solvent used in electrochemistry

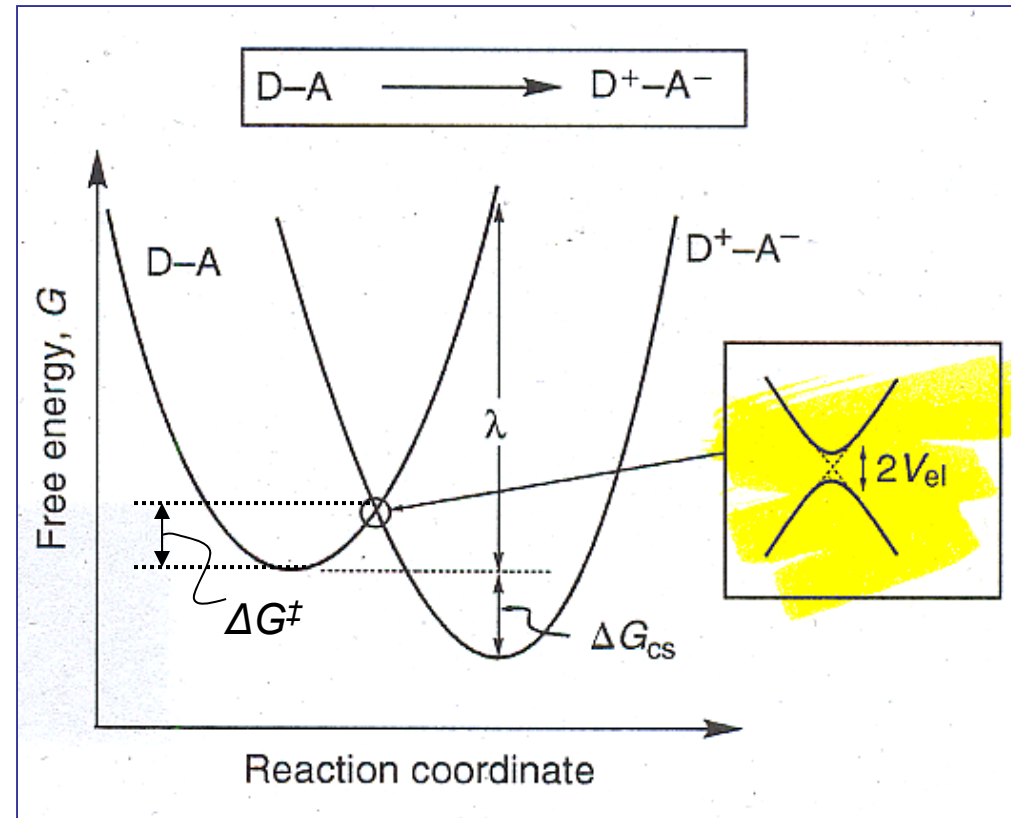
ϵ_s - Dielectric constant of a solvent used in electron transfer system

Electron transfer dynamics

Marcus Theory (The Nobel Prize in Chemistry 1992)



From the analytical geometry of parabolas:
 $\Delta G^\ddagger = (\lambda + \Delta G_{cs})^2 / 4\lambda$



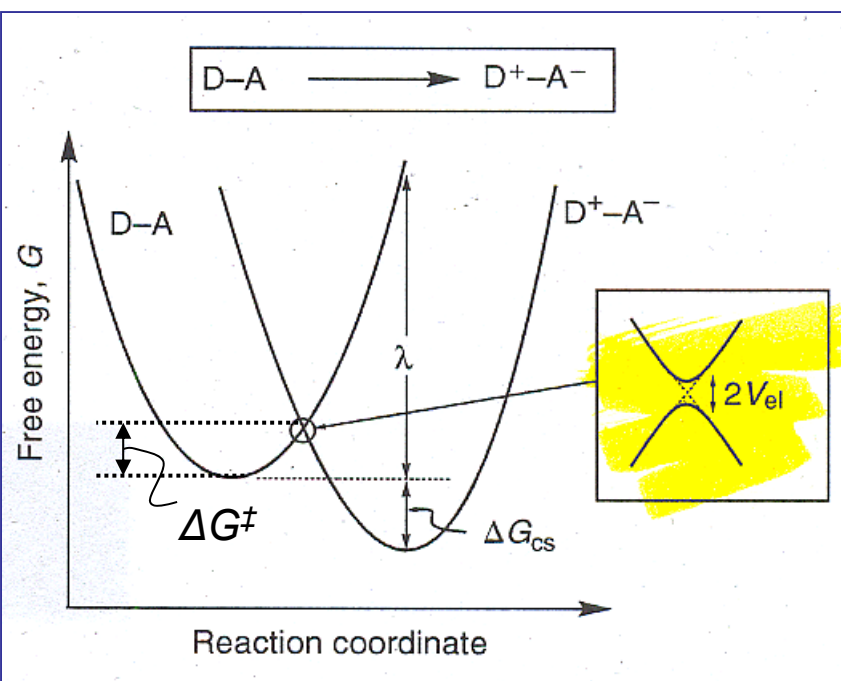
Classical Transition State Theory

$$k_{\text{ET}} = \kappa_{\text{el}} \nu_n \exp \left[\frac{-\Delta G^\ddagger}{k_B T} \right] \quad (4)$$

where ν_n is the frequency of passage (nuclear motion) through the transition state ($D|A$) ‡ ($\nu_n \sim 10^{13} \text{ s}^{-1}$), ΔG^\ddagger is the Gibbs energy of activation for the ET process, κ_{el} is the electronic transmission coefficient, k_B is the Boltzmann constant, and T is temperature. In the classical treatment κ_{el} is usually taken to be unity.

From the analytical geometry of parabolas:

$$\Delta G^\ddagger = (\lambda + \Delta G_{\text{cs}})^2 / 4\lambda$$



Marcus-Hush equation for electron transfer rate

$$k_{\text{et}} = \frac{4\pi^2 |V_{\text{el}}|^2}{h} \left\{ \frac{1}{4\pi\lambda k_B T} \right\}^{1/2} \exp \left(\frac{-(\Delta G_{\text{cs}} + \lambda)^2}{4\lambda k_B T} \right)$$

Three important quantities that affect the magnitude of k_{et} are V_{el} , ΔG_{cs} , and λ , the reorganization energy. The reorganization energy is an important concept in ET theory and is defined as the energy required to distort the reactant and its associated solvent molecules from their relaxed nuclear configurations to the relaxed nuclear configurations of the product and its associated solvent molecules.

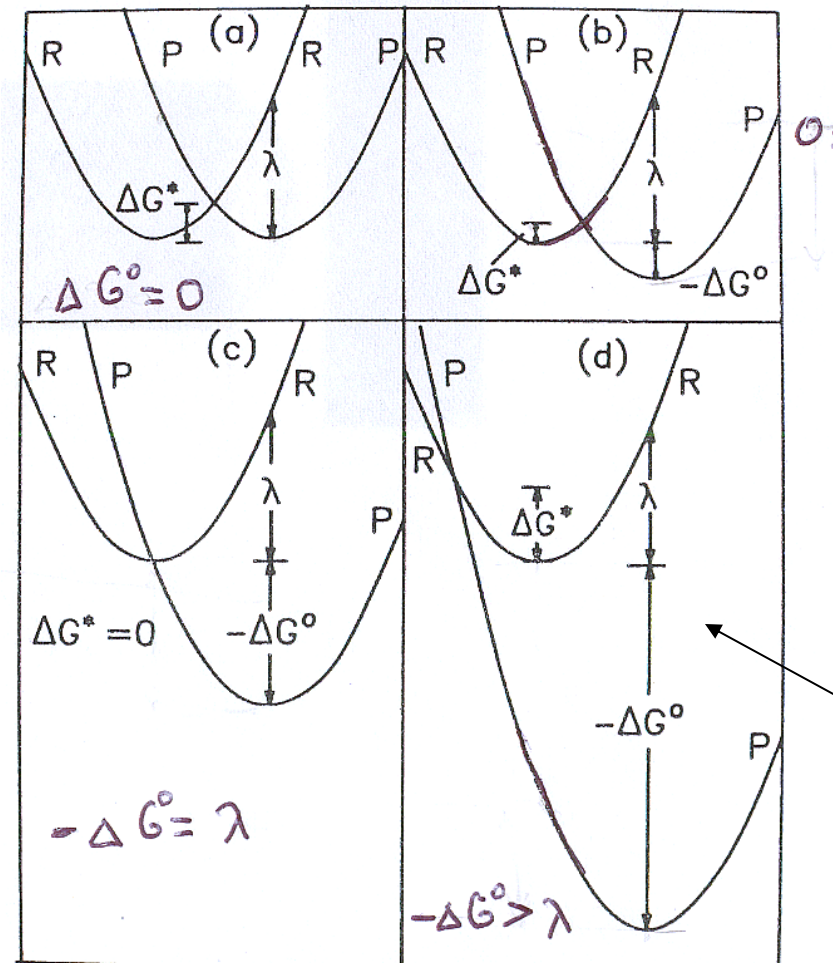
Reorganization Energy

$$\lambda_{\text{total}} = \lambda_{\text{int}} + \lambda_s$$

λ_{int} – inner sphere reorganization energy. Called *intramolecular* reorganization energy. Arises from structural differences between the relaxed nuclear geometries of the reactant and product.

λ_s – outer sphere reorganization energy. Called *solvent* reorganization energy. Arises from differences between the orientation and polarization of the solvent molecules surrounding the reactant and product.

Inverted Region



$$\Delta G^\ddagger = (\lambda + \Delta G_{CS})^2 / 4\lambda$$

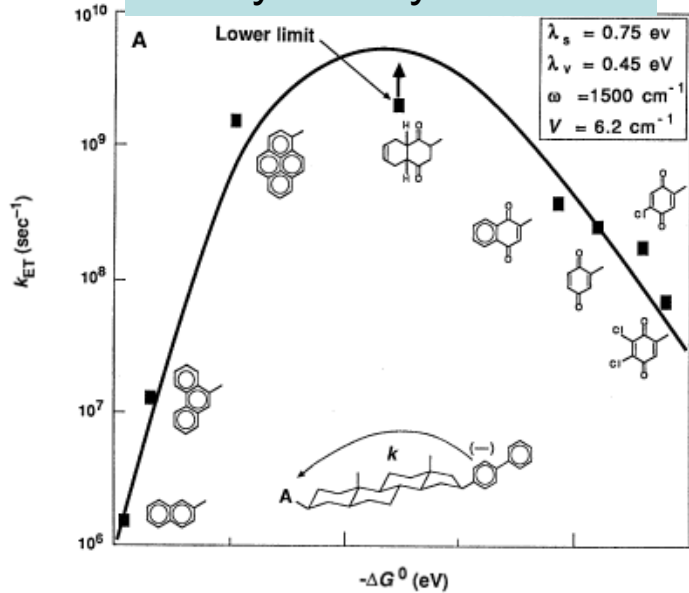
Marcus predicted something completely counter-intuitive:

If there is a really huge driving force for the electron transfer, larger than reorganization energy, the reaction will become slower!

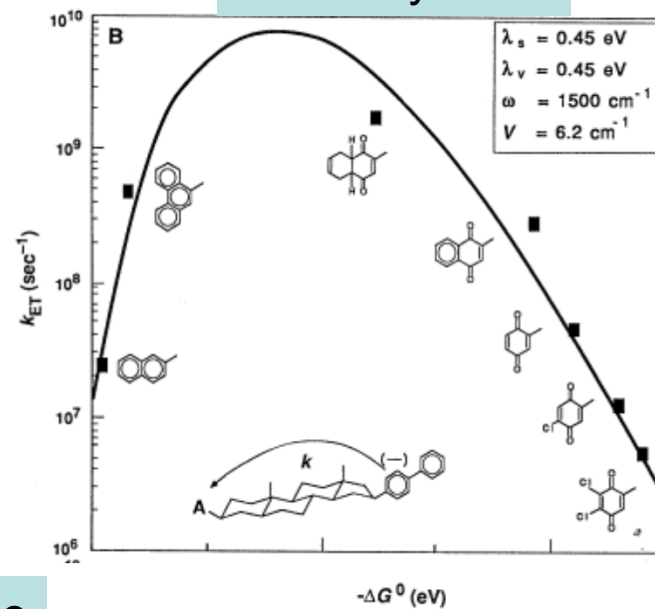
This was the reason that for several years people were skeptical regarding his theory.

Miller and Closs

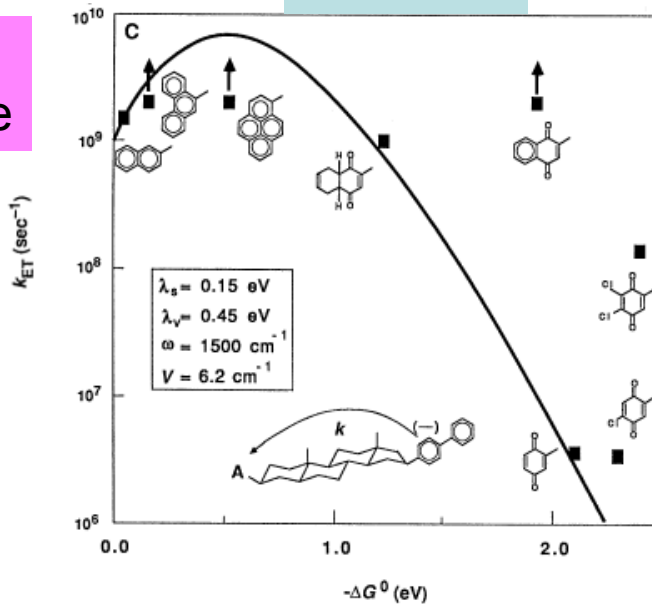
methyltetrahydrofuran



Di-n-butylether



isoctane

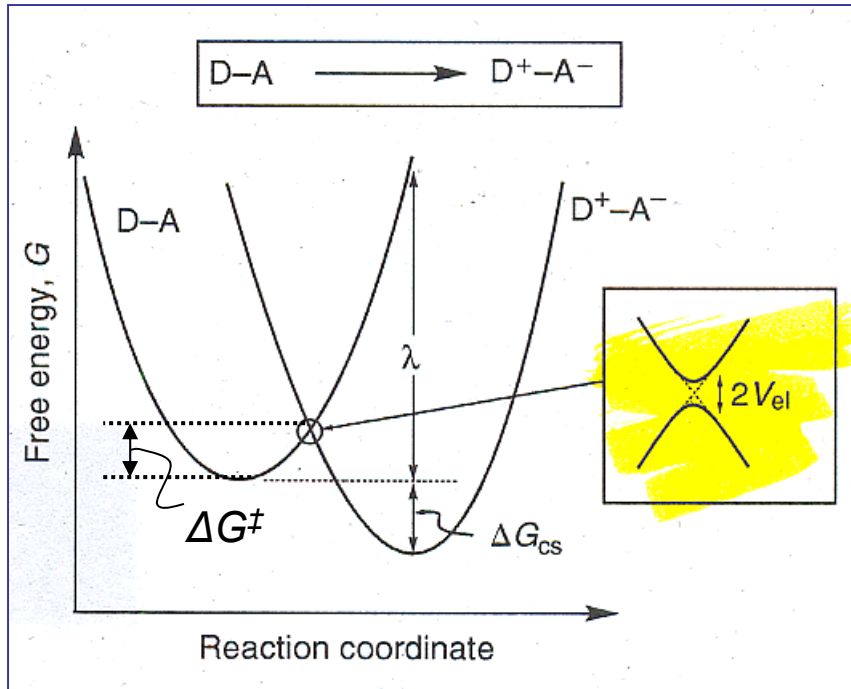


Solvent polarity:
 MTHF > DBE > isoctane

Closs et al.
JACS **1983**, *105*, 670

Closs, Miller,
Science **1988**, *240*, 440.

Electronic coupling



$$k_{et} = \frac{4\pi^2 |V_{el}|^2}{h} \left\{ \frac{1}{4\pi\lambda k_B T} \right\}^{1/2} \exp\left(\frac{-(\Delta G_{cs} + \lambda)^2}{4\lambda k_B T}\right)$$

The matrix element V_{el} (*electronic coupling energy*) scales with the interaction energy between the donor orbital and the acceptor orbital that are associated with the migrating electron. This term depends on the overlap between two orbitals.

V_{el} fall off exponentially with increased interchromophore separation because of decreasing orbital overlap.

Quantum Mechanical Corrections for Marcus Theory: vibronic (phonon) theory

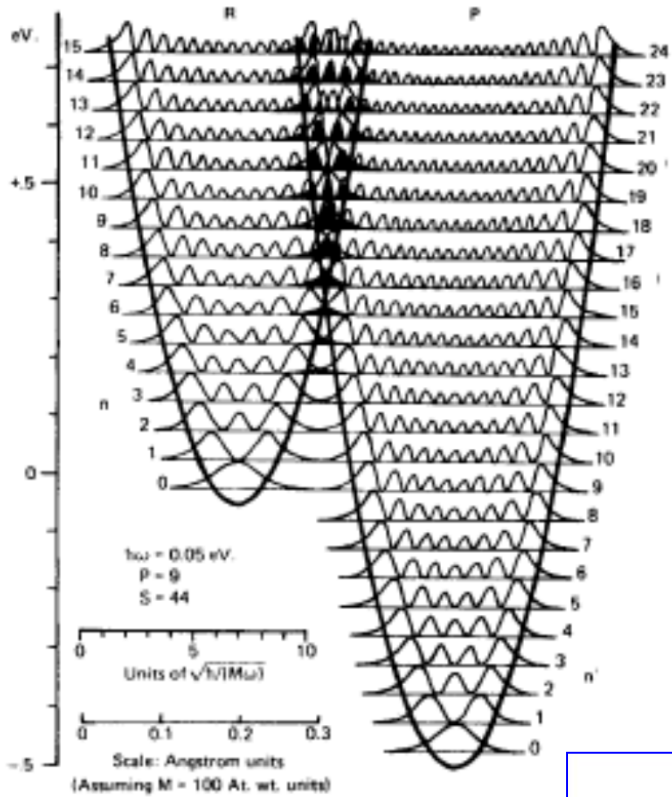
Problems:

- Classical Marcus theory works well only if $V_{el} \geq kT$
- Marcus theory does not predict temperature dependence correctly.
- Marcus theory does not explain electron transfer at very low temperatures.

Conclusion:

The assumption that the barrier should be always crossed is not always holds.

Tunneling should be taken into account.



Vibrational overlap is of primary importance: electron transfer can occur above or below crossing point provided there is good vibrational overlap. Quantum corrections to Marcus theory dealing with vibrations (phonons) were introduced by Jortner and others.

Semiclassical eT theory (Jortner's theory):

$$k_{cs} = \frac{2\pi^{3/2}}{h\sqrt{\lambda_s k_B T}} (V)^2 \sum_{m=0}^{\infty} \frac{e^{-S} S^m}{m!} \exp\left[\frac{-(\lambda_s + \Delta G_{cs} + mh\nu_i)^2}{4\lambda_s k_B T}\right]$$

with the electron-vibronic (phonon) coupling $S = \lambda_i/h\nu_i$. Here ν_i is the average skeletal (IR)-vibration (in general between 300 and 2300 cm⁻¹). The “Σ” term indicates a summation over all “m” levels.



Barbara et al. describe it well

Factors that Influence Electron Transfer

Electron transfer rates depend on

- Driving force ΔG^0
- Reorganization energy λ
- Solvent (ΔG^0 , λ)
- Electronic coupling V_{el}
- Distance between donor (D) and acceptor (A) (ΔG^0 , λ , V_{el})
- Orientation of D relative to A (V_{el})
- Temperature

Distance dependence

V_{el} is proportional to $e^{-0.5\beta r}$

k_{ET} is proportional to $e^{-\beta r}$

β = damping factor

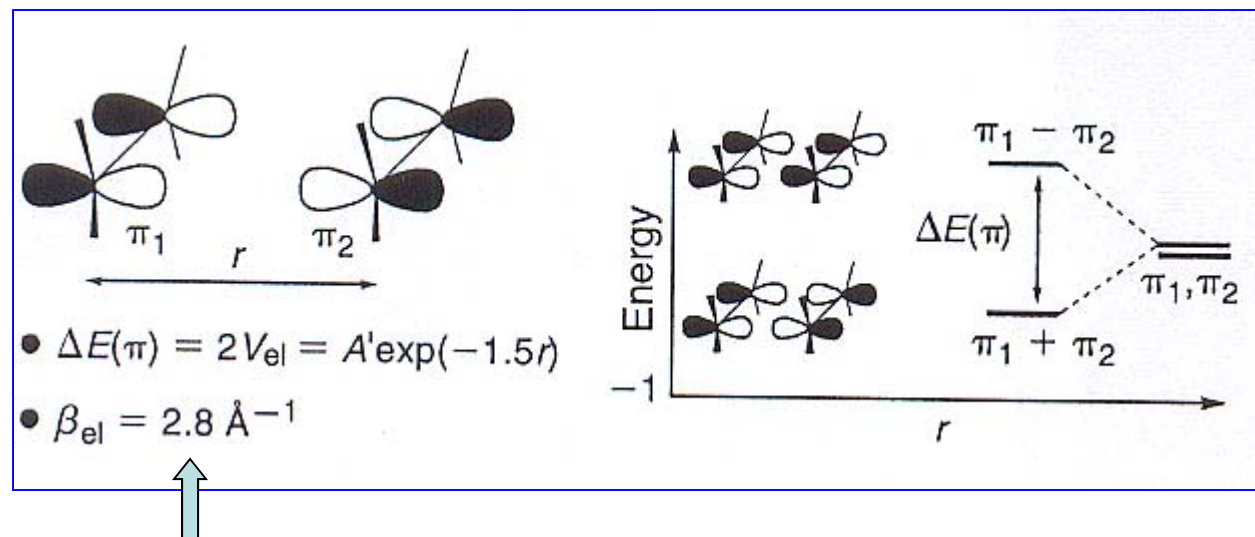
r = distance

Large β – significant falloff of rates with distance

Small β – rates are almost independent of distance
(molecular wire)

Through-space distance dependence

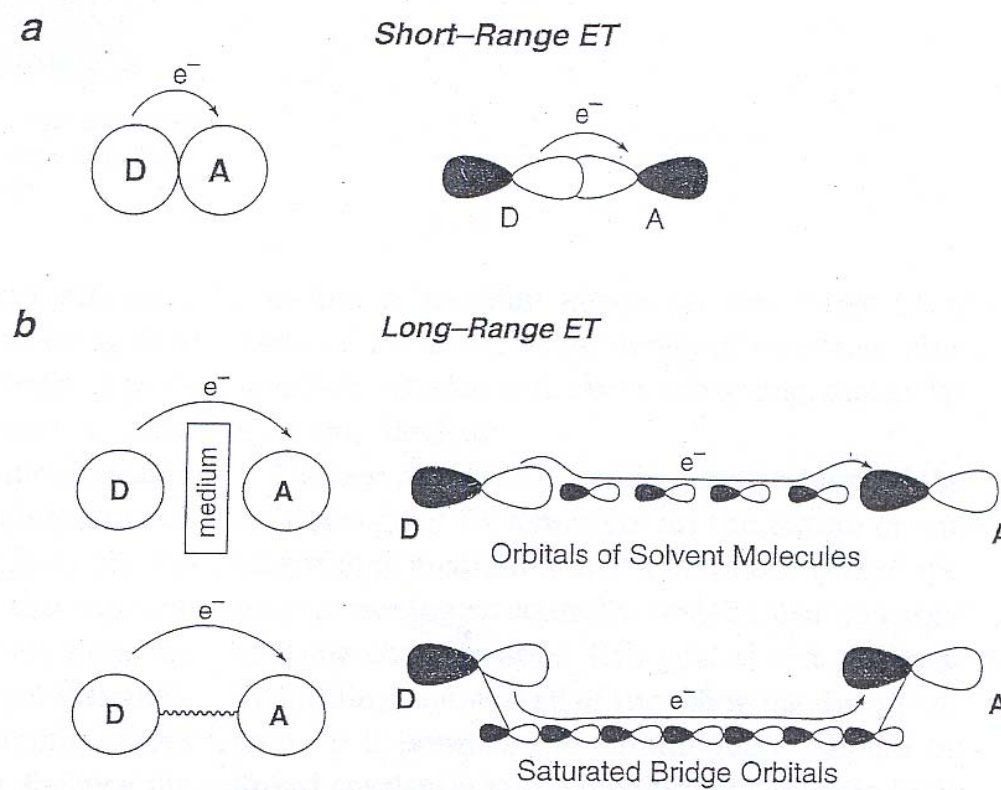
In the absence of any intervening medium (vacuum) the electronic coupling depends on direct through space overlap between the active orbitals of the donor and acceptor. Calculation for two ethylene molecules:



Large value for damping factor, which means that the eT rate occurring by a through-space mechanism should be attenuated by a factor as large as 20 per 1Å

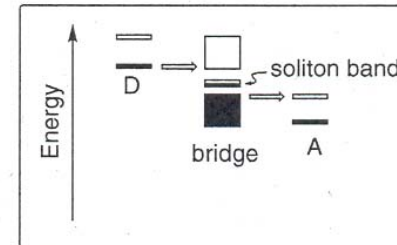
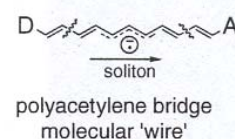
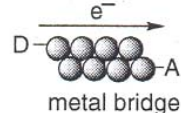
Bridge between donor and acceptor: how it influences eT

Figure 2. (a) Short-range ET. The donor and acceptor orbitals overlap strongly and ET takes place by a direct, through-space mechanism. (b) Long-range ET. Direct overlap between the donor and acceptor orbitals is negligible and ET occurs by an indirect mechanism involving electron tunnelling through the orbitals of the intervening medium, e.g. solvent molecules (upper) or a covalently linked saturated bridge (lower).

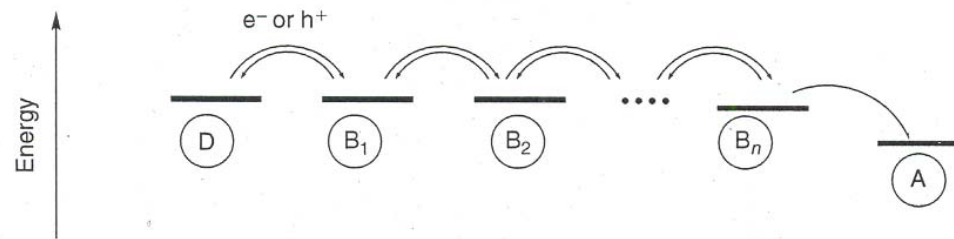


Hopping vs Superexchange

(a) Electrically conducting bridges: electron transport

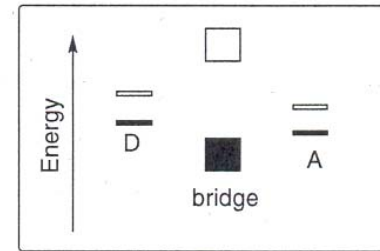
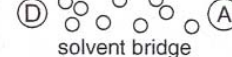
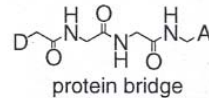
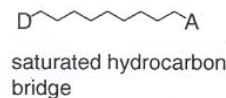


(b) Charge-hopping bridges: electron transport



Hopping: charges
reside on the bridge

(c) Electrically insulating bridges ('saturated' bridges): electron transfer

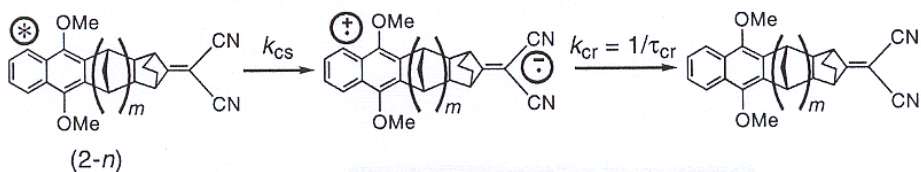


Superexchange: the bridge mediates electron transfer,
although the charges never reside on it. One can say
that the electron tunnels through the bridge.

Superexchange example: saturated bridge

(2-4)		$R_e (\text{\AA})$	4.6
(2-6)			6.8
(2-8)			9.4
(2-9)			10.9
(2-10)			11.5
(2-12)			13.5
(2-13)			14.2

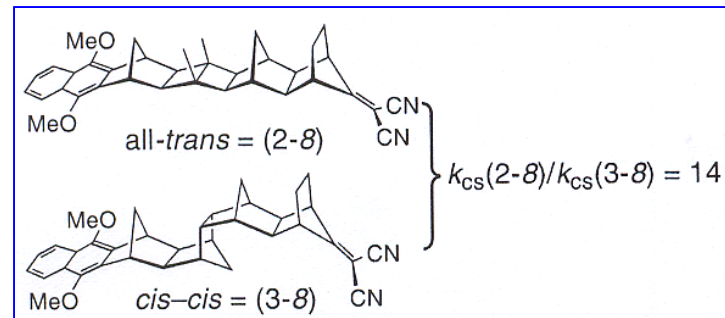
Table 1. Rate data for photoinduced charge separation and subsequent charge recombination in the dyads (2-n)



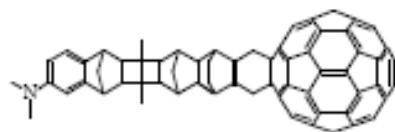
System	Charge separation rates $k_{cs} [10^8 \text{ s}^{-1}]^A$		Mean lifetime towards charge recombination $\tau_{cr} [\text{ns}]^B$
	Fluorescence measurements ^[68,70]	Pump-probe measurement ^[81]	
(2-4)	$\gg 5000$	28 000	—
(2-6)	3000	4890	0.5
(2-8)	670	1160	2.5
(2-9)	250	647	—
(2-10)	120	180	43
(2-12)	13	—	297
(2-13)	1.2	—	1050

^A Measured in THF at 20°C. ^B From time-resolved conductivity measurements in 1,4-dioxane.^[67,77,79,80]

$$\beta \sim 1$$



Why is there superexchange?



The charge separation involves an interaction between the orbitals **a** and **d**, while charge recombination involves interactions between **a*** and **d**.

Experimental observations show that the ratio between the rates of charge separation and charge recombination for this system is in fact more than three orders of magnitude ($k_{cs}/k_{cr} = 1400$).



Fig. 16. Visualization of orbital *a* of the donor-bridge-fullerene(acceptor) system in 'side' (left) and 'top' (right) view, obtained from AM1 calculations, using a value of 0.001 electrons/au³.

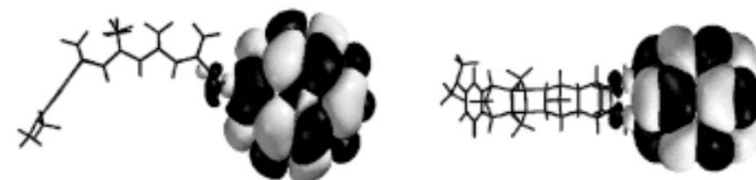
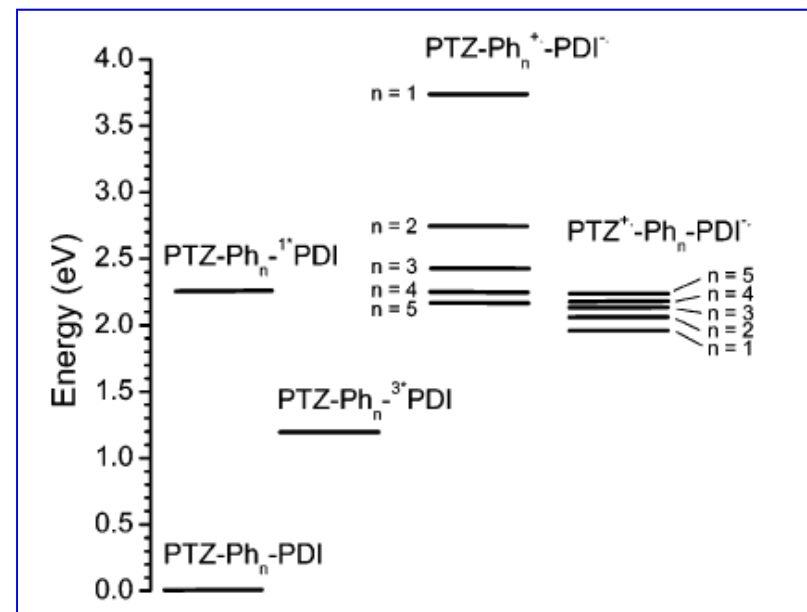
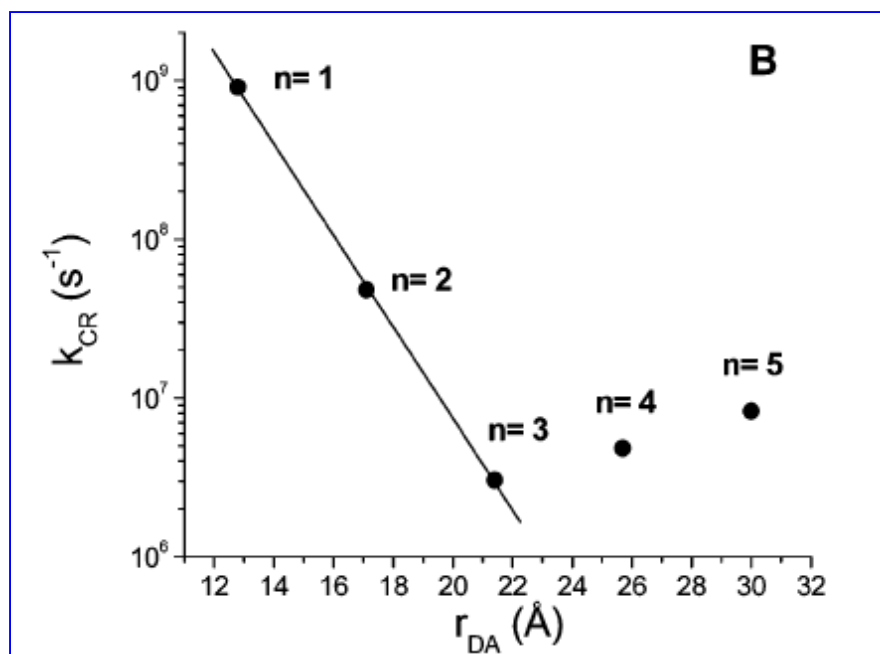
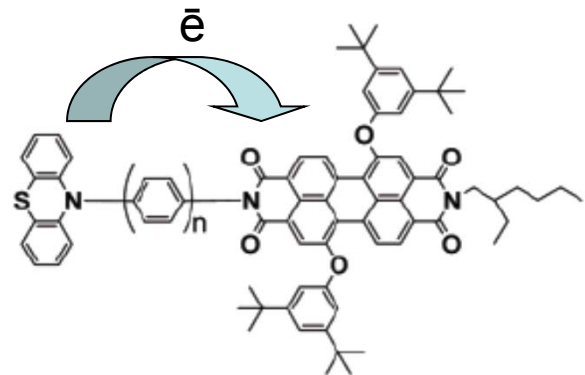


Fig. 17. Visualization of orbital *a** of the donor-bridge-fullerene(acceptor) system in 'side' (left) and 'top' (right) view, obtained from AM1 calculations, using a value of 0.001 electrons/au³.



Fig. 18. Visualization of *d* of the donor-bridge-fullerene(acceptor) system in 'side' (left) and 'top' (right) view, obtained from AM1 calculations, using a value of 0.001 electrons/au³.

Hopping and molecular wires



The oligomeric *p*-phenylene bridge acts as a molecular wire for the charge recombination reaction of $\text{PTZ}^{+ \cdot}-(\text{Ph})_n-\text{PDI}^{\cdot -}$ when $n \geq 4$. **Switch in the mechanism from superexchange to hopping** takes place when $n \geq 4$.

Wasielewski, Ratner et al.

Summary of β values

Saturated hydrocarbon bridges

$$\beta \sim 0.75\text{-}0.98 \text{ \AA}^{-1}$$

Unsaturated, unconjugated hydrocarbon bridges

$$\beta \sim 0.5 \text{ \AA}^{-1}$$

Conjugated hydrocarbon bridges

$$\beta \sim 0.04\text{-}0.4 \text{ \AA}^{-1}$$

Proteins

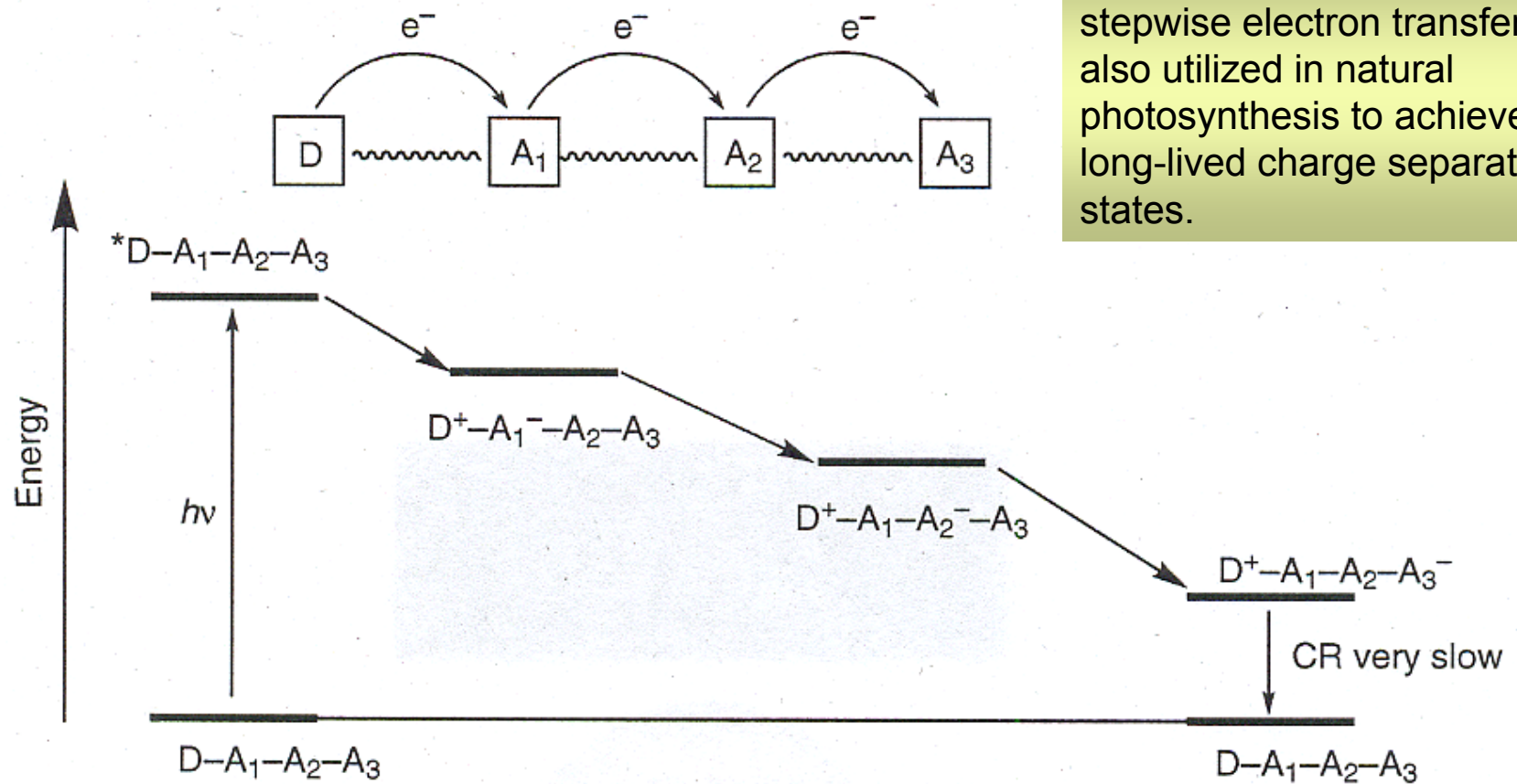
$$\beta \sim 0.8\text{-}1.4 \text{ \AA}^{-1}$$

Duplex DNA

$$\beta \sim 0.6\text{-}1.0 \text{ \AA}^{-1}$$

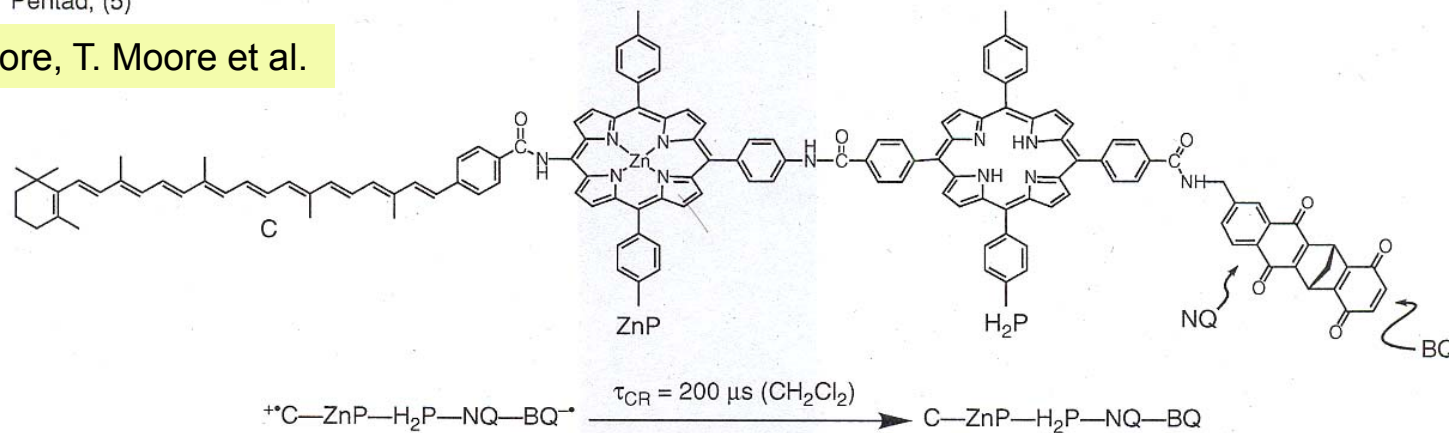
Long-lived charge separation

Long-lived charge separation states. Cascade: gradient of redox centers



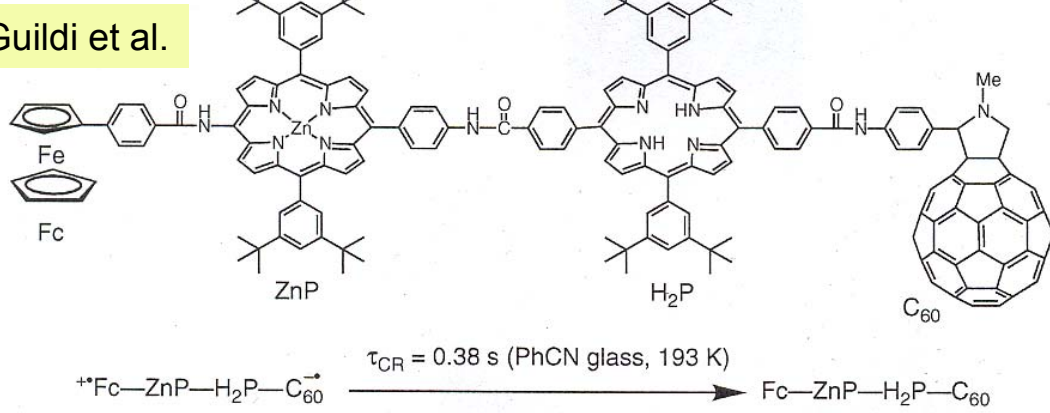
Pentad, (5)

Gust, A. Moore, T. Moore et al.



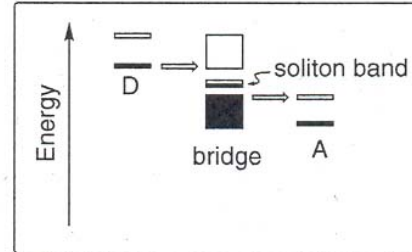
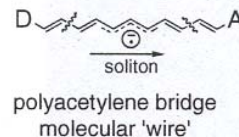
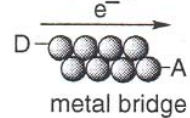
Tetrad, (6)

Imahori, Guildi et al.

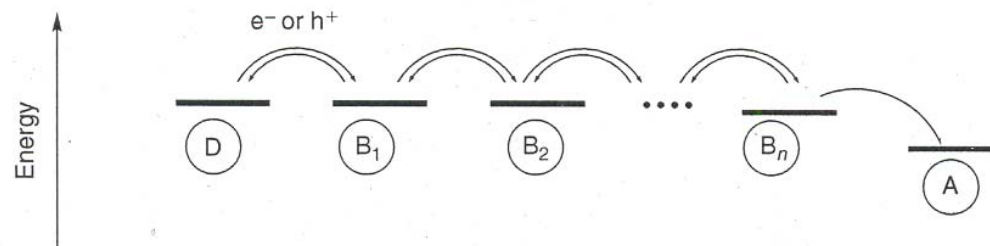


Hopping vs Superexchange

(a) Electrically conducting bridges: electron transport

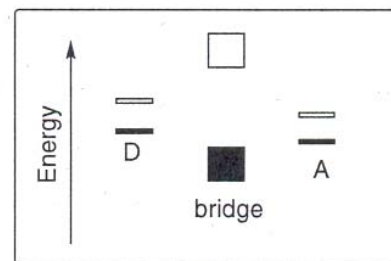
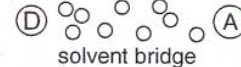
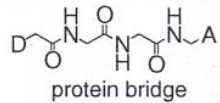
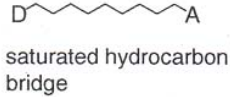


(b) Charge-hopping bridges: electron transport



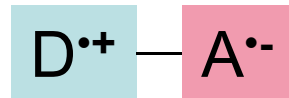
Hopping: charges reside on the bridge

(c) Electrically insulating bridges ('saturated' bridges): electron transfer



Superexchange: the bridge mediates electron transfer, although the charges never reside on it. One can say that the electron tunnels through the bridge.

Electron transfer and triplets



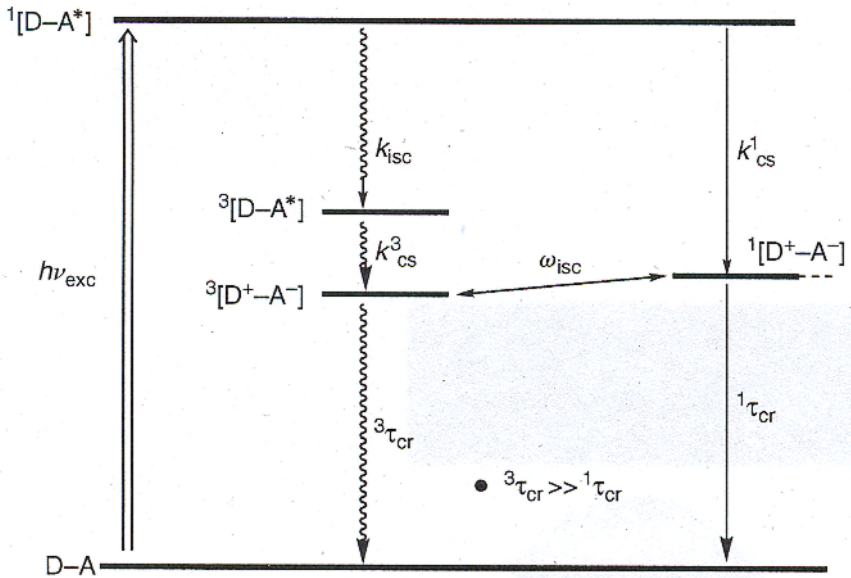
Radical ion pair

Recognizing that a CT state can be described in terms of a radical ion pair (RIP) implies that such a state can in principle adopt either a singlet or a triplet spin configuration (${}^1\text{CT}$ resp. ${}^3\text{CT}$). The energy gap separating ${}^1\text{CT}$ and ${}^3\text{CT}$ is given by $2J$ where J is the spin–spin exchange integral. Qualitatively it is evident that the absolute value of J will decrease with increasing distance between radical sites.

Triplet states for long CS lifetime

M. N. Paddon-Row

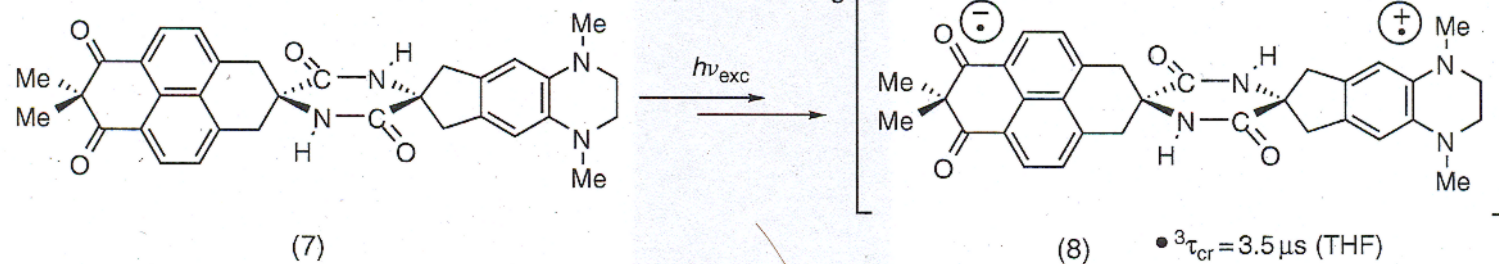
(a)



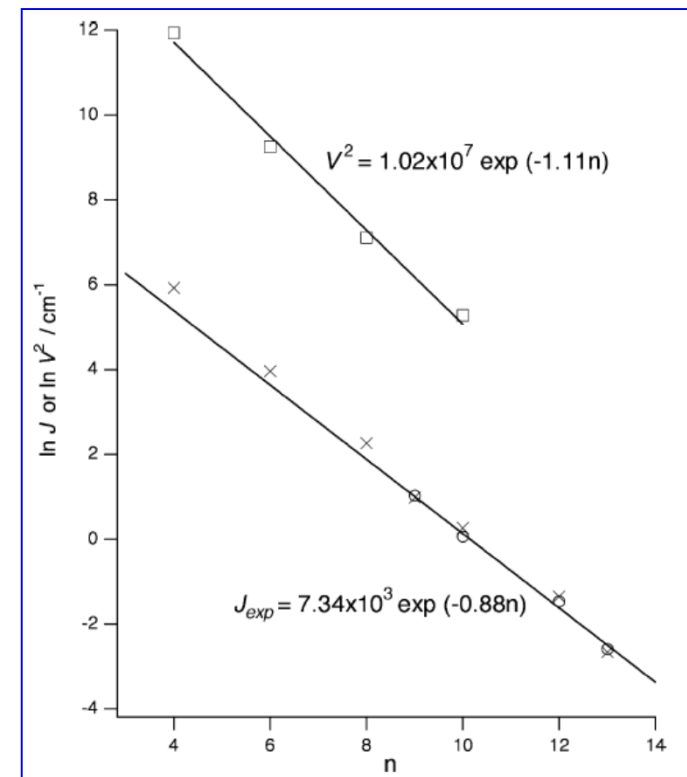
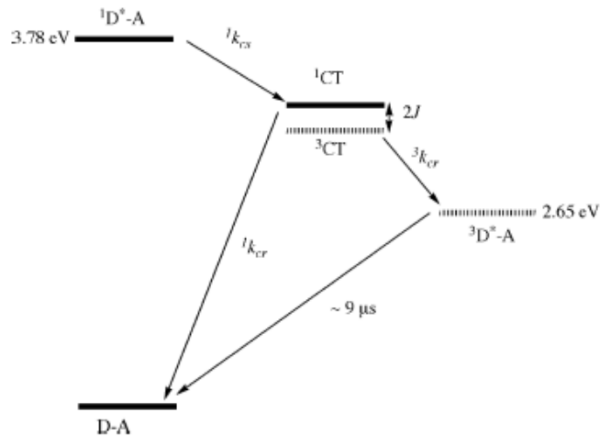
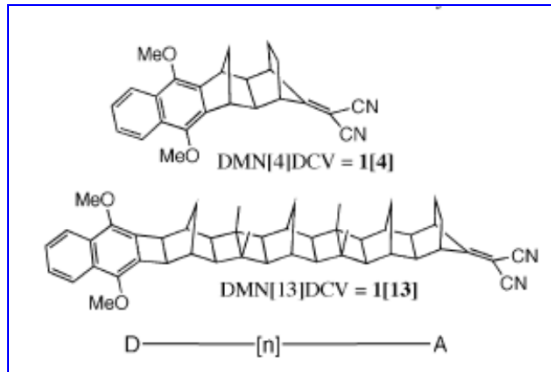
Conditions for populating the triplet CS state

- $k_{isc} \gg k^1_{cs}$
- $E(^3[D-A^*]) > E(^3[D^+-A^-])$

(b)



Example



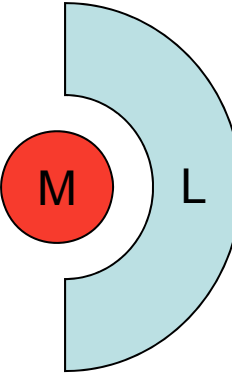
Paddon-Row, Verhoeven et al.

<i>n</i>	τ_{cs} (ps) ^a	Φ_{CT}^{b}	τ_{cr} (ns) ^c	$\Phi(^3D^*)^{d}$	$V(\text{cm}^{-1})^{e}$	$J_{\text{exp}}(\text{cm}^{-1})$	$J_{\text{calc}}(\text{cm}^{-1})^{f}$
4	0.36	1.00	0.08	0.00	392	—	374.4
6	2.05	1.00	0.5	0.03	102	—	52.8
8	8.62	1.00	2.5	0.09	35	—	9.6
9	15.5	1.00	—	—	—	2.8 ^g	2.68
10	55.5	0.99	43	0.37	14	1.06 ^h	1.30
12	770	0.91	297	0.64	—	0.23 ^h	0.258
13	1070 ⁱ	0.87	1050	-	—	0.075 ^g	0.070

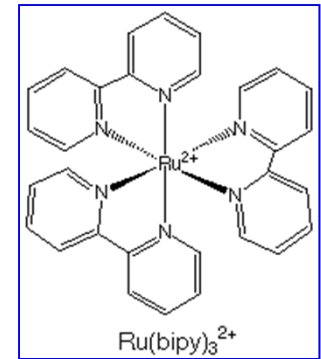
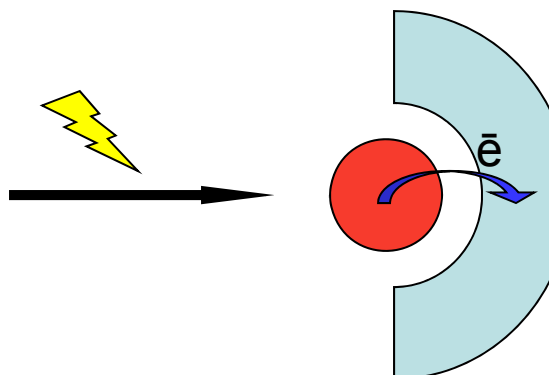
Charge transfer in metal complexes

MLCT

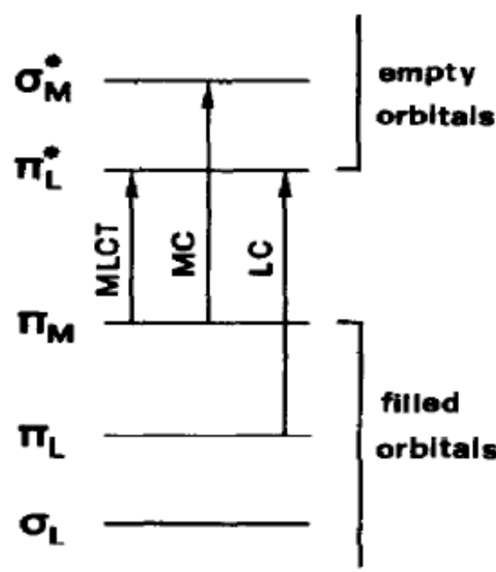
LUMO
(π^* of the ligand)



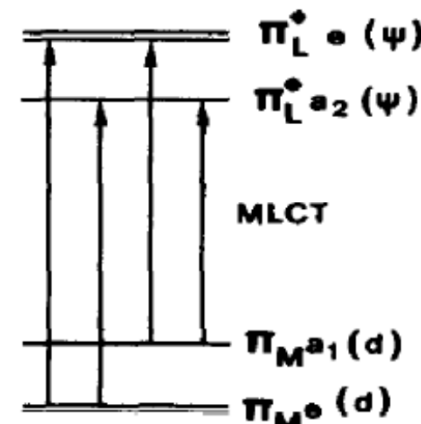
HOMO
(metal based)

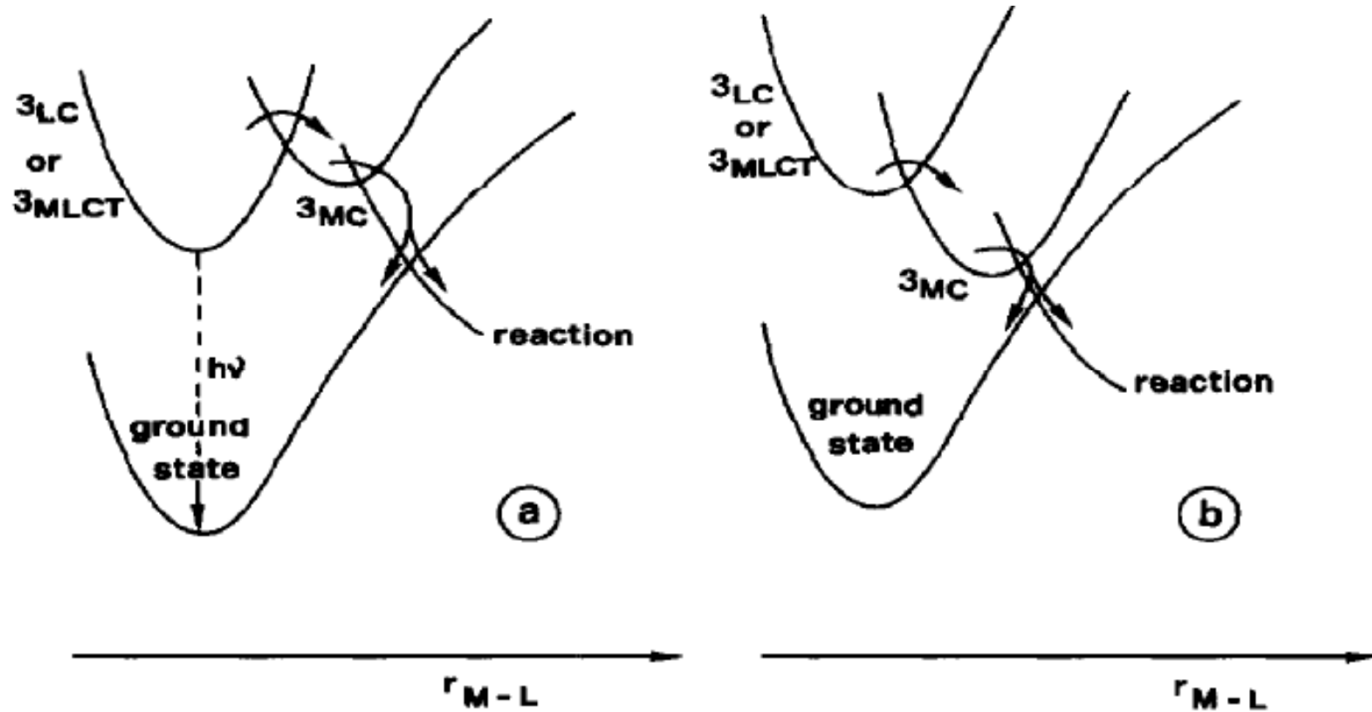


a



b





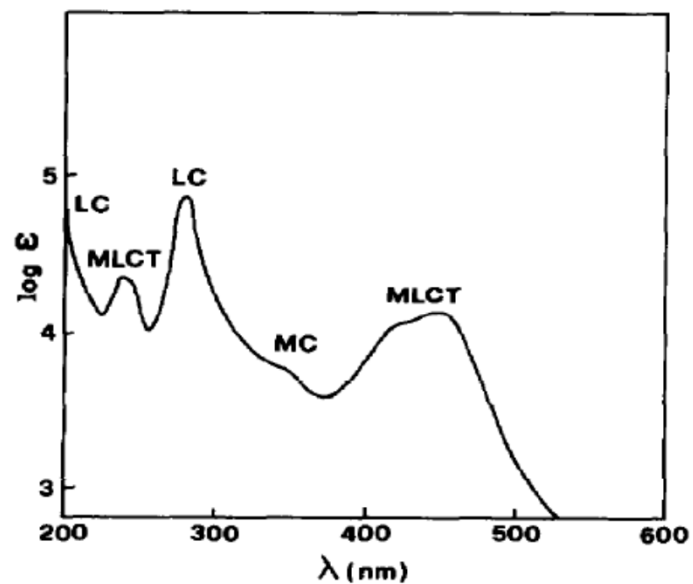
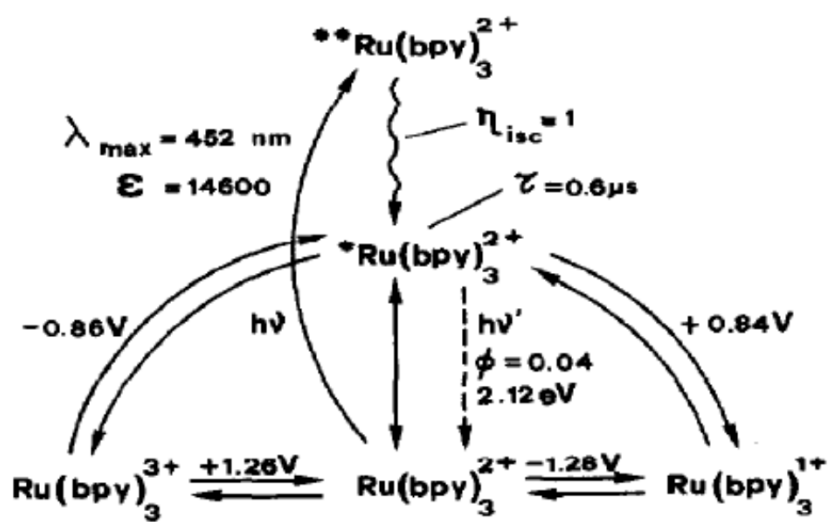
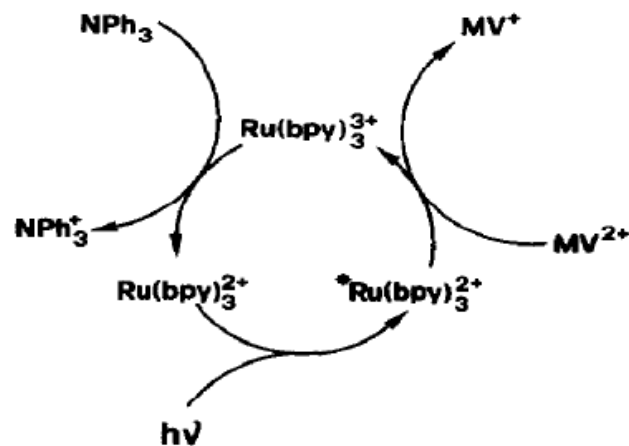


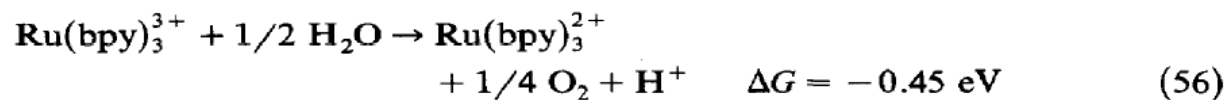
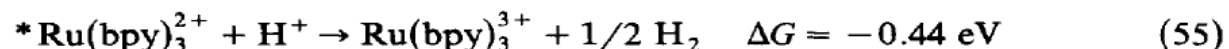
Fig. 17. Electronic absorption spectrum of $\text{Ru}(\text{bpy})_3^{2+}$.

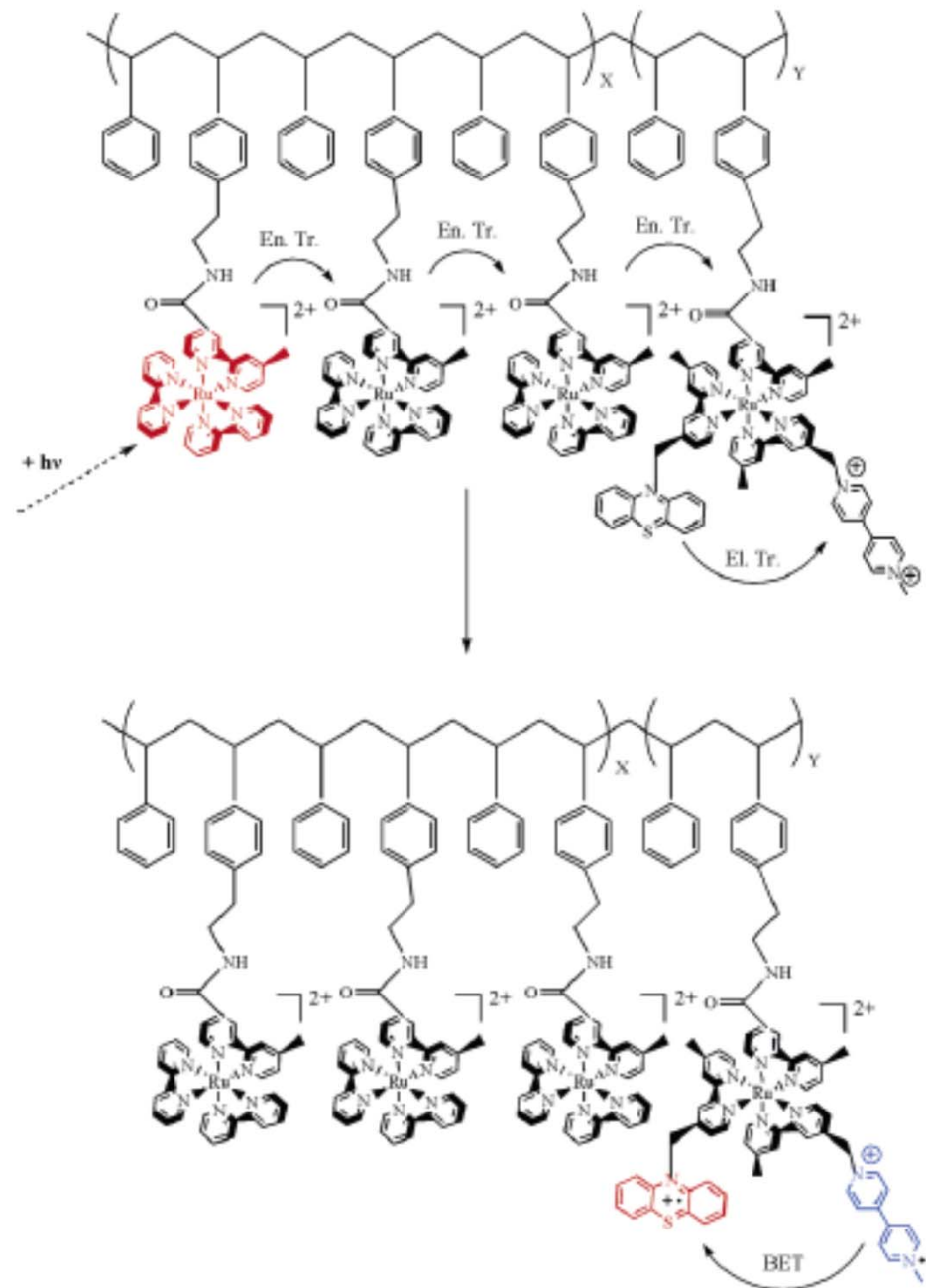


Sensitization

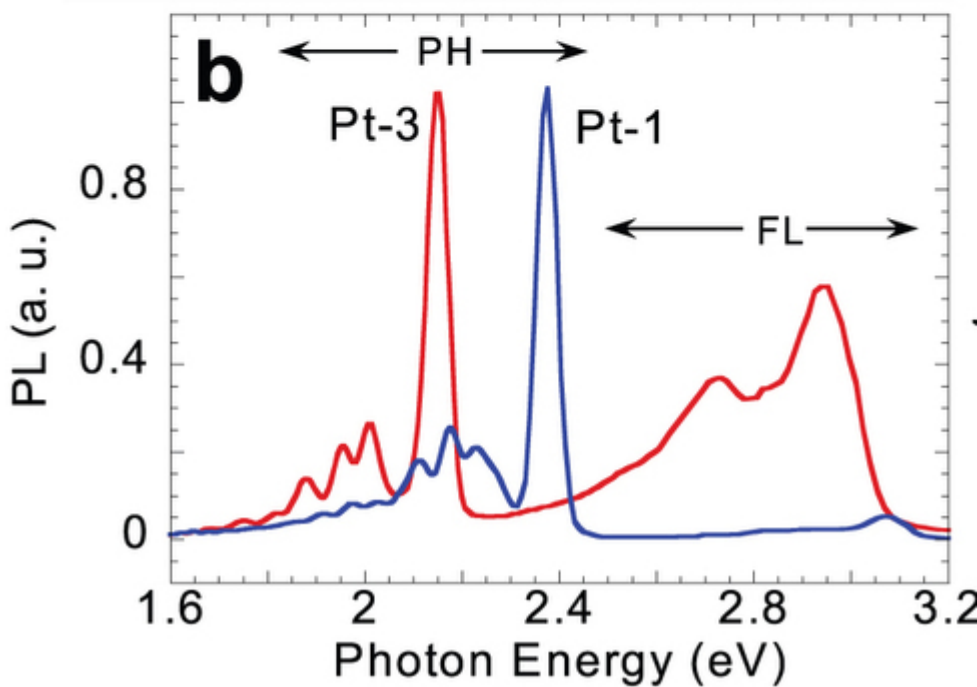
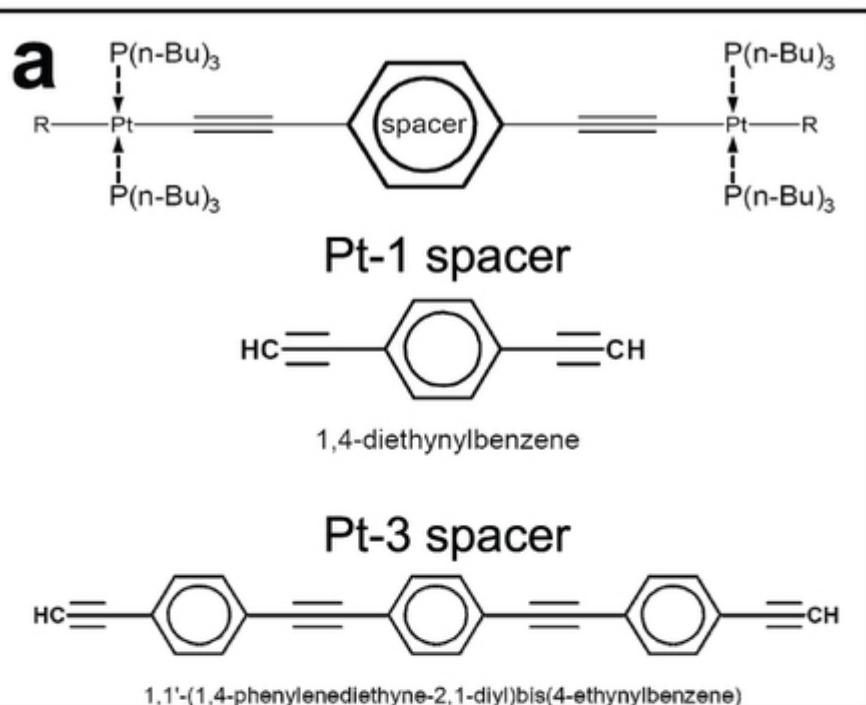


This reaction, which in the dark is endergonic by 1.23 eV, could be driven by visible photons which, however, are not absorbed by water. In principle, $\text{Ru}(\text{bpy})_3^{2+}$ can play the role of LAS even in this case. At pH 7, the energetics of the relevant steps are as follows:





Fleming et al.



OPEN

SUBJECT AREAS
ORGANIC
NONLINEAR OPTICS
CHEMICAL PHYSICS
MOLECULAR ELECTRONICS

Received
24 April 2013

Accepted
22 August 2013

Published
13 September 2013

Correspondence and
requests for materials
should be addressed to
Z.V. (zv@physics.
utah.edu)

Ultrafast intersystem-crossing in platinum containing π -conjugated polymers with tunable spin-orbit coupling

C.-X. Sheng^{1,2*}, S. Singh^{1*}, A. Gambetta^{1,3†}, T. Drori¹, M. Tong¹, S. Tratikov² & Z. V. Vardeny¹

¹Department of Physics & Astronomy, University of Utah, Salt Lake City, Utah 84112, USA, ²School of Electronic and Optical Engineering, Nanjing University of Science and Technology, Nanjing, Jiangsu, 210094, China, ³Theoretical Division, Center for Nonlinear Studies (CNS), and Center for Integrated Nanotechnologies (CINT), Los Alamos National Laboratory, Los Alamos, New Mexico 87545, USA.

The development of efficient organic light-emitting diodes (OLED) and organic photovoltaic cells requires control over the dynamics of spin sensitized excitations. Embedding heavy metal atoms in π -conjugated polymer chains enhances the spin-orbit coupling (SOC), and thus facilitates intersystem crossing (ISC) from the singlet to triplet manifolds. Here we use various nonlinear optical spectroscopies such as two-photon absorption and electroabsorption in conjunction with electronic structure calculations, for studying the energies, emission bands and ultrafast dynamics of spin photoexcitations in two newly synthesized π -conjugated polymers that contain an intrachain platinum (Pt) atoms separated by one (Pt-1) or three (Pt-3) organic spacer units. The controllable ISC rate modulates the intensity ratio of the phosphorescence and fluorescence emission bands, with potential applications for white OLEDs.

In this work two Pt-containing polymers (namely Pt-1 and Pt-3) with different organic spacer length in between each two adjacent intrachain Pt atoms were synthesized and extensively studied using a variety of NLO spectroscopies that include electroabsorption, two-photon absorption, and ultrafast and steady state photomodulation. The NLO spectra were compared to the absorption and luminescence spectra. From quantum chemistry calculation and the NLO measurements we conclude that the lowest singlet state in Pt-1 is a Metal-to-Ligand Charge Transfer (MLCT) state, which lies below the lowest $\pi-\pi^*$ exciton; however, the order is reversed in Pt-3. Surprisingly, the primary photoexcitations in both polymers are singlet $\pi-\pi^*$ excitons, irrespective of the excited state order. We note, however that the electron in the MLCT state is localized on the Pt atom center orbital. Consequently the MLCT states have relatively large SOC and their energy is practically independent on the linker length. In contrast the energy of the $\pi-\pi^*$ transitions substantially depend on the linker length. Because of the π -electron delocalization within the π -conjugated linker, the $\pi-\pi^*$ $1B_u$ state has relatively weak SOC, which is further reduced for longer linker. This rationalizes our experimental results of the way the intrachain Pt atom influences the ISC rate in both Pt-1 and Pt-3.

